LETTER

Use of solution-processed zinc oxide to prevent the breakdown in silver nanowire networks

IOP Publishing
Letters
Nanotechnology
Nanotechnology 31 (2020) 18LT01 (7pp)
https://doi.org/10.1088/1361-6528/ab6fe4

Letter

Use of solution-processed zinc oxide to prevent the breakdown in silver nanowire networks

Haoran Yu[1,2], Ning Jin[1,3], Zhenguo Wang[2], Jian Lin[2,3], Junfeng Wei[2], Qun Luo[2] and Chang-Qi Ma[2]

[1] Key Laboratory of Electromagnetic Wave Information Technology and Metrology of Zhejiang Province, College of Information Engineering, China Jiliang University, Hangzhou, 310018, People's Republic of China
[2] Printable Electronics Research Centre, Suzhou Institute of Nano-Tech and Nano-Bionics, Chinese Academy of Sciences, Suzhou Industrial Park, Suzhou, Jiangsu Province, 215123, People's Republic of China

E-mail: jinning1117@cjlu.edu.cn and jlin2010@sinano.ac.cn

Received 25 November 2019, revised 22 December 2019
Accepted for publication 24 January 2020
Published 17 February 2020

Abstract

The electrical breakdown is a bottleneck preventing AgNW networks from being used in high-current electronics such as transparent heaters or similar applications. The process of failure confirms that Joule-heating plays a key role in the formation of cracks perpendicular to the voltage direction. To improve the transfer of Joule heating, solution-processed ZnO nanoparticles were deposited on a gravure printed AgNW random network with good transparency. The AgNW-ZnO nanocomposites show better heating uniformity at higher temperatures because of their improved thermal conductivity. A 57.7% higher power density was obtained without failure, as well as the improved maximum average temperature rise from 72.2 °C to 97.9 °C, after the AgNW was composited with ZnO. This work opens up a new method to study AgNW failures for applications in high-current electronics.

Supplementary material for this article is available online

Keywords: Joule heating, cascading failure, silver nanowire, electrical breakdown, zinc oxide, nanocomposites

(Some figures may appear in colour only in the online journal)

1. Introduction

Transparent conductive networks based on silver nanowires (AgNWs) have been used widely in low-current applications including touch panels [1], organic light-emitting diodes [2] and solar cells [3] due to their excellent electrical conductivity, flexibility and transparency. The AgNWs can be deposited to form random networks by slot die [4], spray [5] and Mayer-rod techniques [6], as well as inkjet [7] or gravure printing [8] with patterns. However, the multiple electrical breakdowns of AgNW networks [9] have been reported in high-current electronics because of local Joule heating [10] forming cracks perpendicular to the voltage direction [11]. Additionally, AgNWs with smaller diameter are widely used for their improved connectivity and conductivity at high transmittance [12], though their degradation was also accelerated [13]. To prevent the failure of AgNW transparent heaters, TiO_2 [11], GO [13], AZO [14] and ZnO [15] have been used to improve the stability. These results were usually explained by means of the hindered atomic diffusion caused by the oxide layers [16]. Since

[3] Authors to whom any correspondence should be addressed.

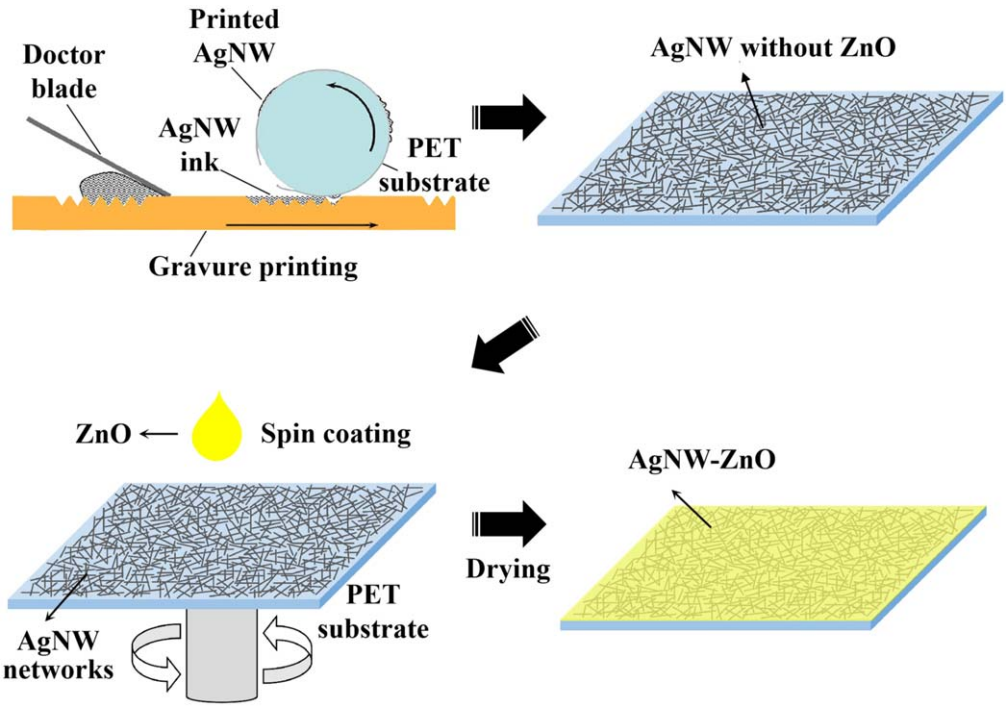

Figure 1. Schematic diagram of the PET/AgNW and PET/AgNW/ZnO fabrication process.

the ZnO material has been widely reported for electron injection/transport layer [17], photo-transistor [18, 19], nanogenerator [20], sensor [21] and composite electrodes [3], the discovery of better stability provides a new method for potential application in transparent electrodes or circuits with higher current. However, considering that heat dissipation affects resistance in printed silver nanoparticles [22], it is necessary to study whether the high thermal conductivity of oxides such as ZnO [23] plays a key role in Joule heating uniformity and AgNW stability. In this letter, solution-processed ZnO was used to fabricate nanocomposites with a gravure printed AgNW random network. The samples were studied as transparent thin-film heaters for heating uniformity and failure inhibition.

2. Experiment

AgNW (about 25 nm diameter, 20 μm length, 5 mg ml^{-1}) aqueous dispersion was purchased from Gu's New Material. It was diluted with isopropyl alcohol with a volume ratio of 1:1, and gravure printed onto PET substrate with a Labratester with a printing speed of 60 mm s^{-1}, as shown in figure 1. The printed PET/AgNW film was cut into 3.5 cm × 2.5 cm sections after 130 °C heating for 10 min. Some of the PET/AgNW pieces were spin-coated (2000 rpm/50 s) using a methanol solution of 10 mg ml^{-1} ZnO nanoparticles, which were named PET/AgNW/ZnO. Then, the samples were annealed at 130 °C for a further 10 min. 0.5 cm × 2.5 cm electrodes were screen-printed using silver paste to the ends of the samples to fabricate the transparent heaters.

The scanning electron microscope (SEM) and optical transmittance were characterized using a Hitachi S-4800 and Lambda 750 UV/vis spectrometer respectively. A Keithley 2400 source-meter was used to measure currents interfaced with a computer running the LabVIEW program. An FLTR T530 infrared camera was used to measure the temperature of the heated film in real-time. The simulation of voltage drops in the equivalent circuit was performed using the Multisim software from National Instruments.

3. Results and discussion

To understand the formation of cracks perpendicular to the voltage direction in a failed AgNW network, the current and surface temperature of AgNW during the breakdown processes were recorded with a Keithley 2400 source-meter and infrared camera. The hot-spot with maximum temperature was found to move with a track (figure 2(b)) overlapping the crack formed during the process of breakdown (figure 2(c)) with variable speed. The infrared video also confirms that higher temperature plays a key role in the failed cracks of AgNW. The maximum temperature in the short periods I, shown in figure 2(a), increases from 89.97 °C to 130.08 °C in 4.466 s, while the whole average temperature of the sample drops from 74.73 °C to 73.98 °C. The resistance rises from 93.9 Ω to 144.1 Ω in 3.0 s during periods II. The maximum temperature between the two periods is higher than the superior measuring limit (130.2 °C) and lasts for about 80 s.

To explain the hot-spot movements during the failure process, the AgNW network can be modeled as an equivalent circuit diagram with interconnected conducting resistances (figure 3(a)). A simplified cascading failure model containing 13 same resistors (figure 3(b)) is used to explain the hot-spot movement. The electrical power of a resistor can be

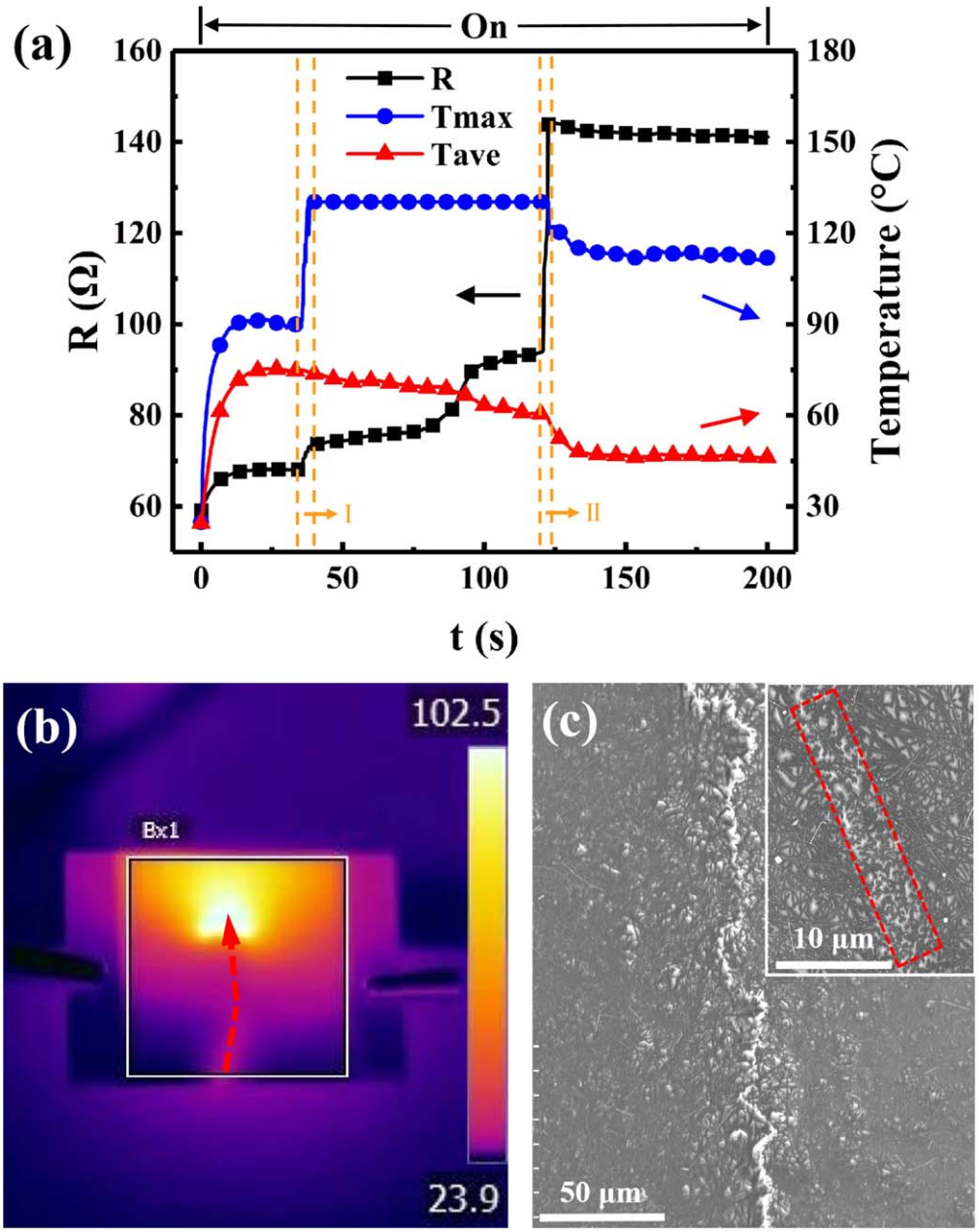

Figure 2. (a) The maximum and average temperature as well as the resistance of a sample without ZnO. (b) A screen shot from the video with the movement trajectory of the hot spot during the breakdown. (c) SEM image of failed AgNW with a crack, the insert shows the crack in detail.

calculated by the equation as follow,

$$P = U^2/R \quad (1)$$

Where P is the electrical power, U is the voltage drop across the resistor, and R is the resistance. The results show that the resistors in the bias direction have the same voltage and power when the V_{CC} (11 V) is applied because of the same voltage drops.

However, if a resistor (R_{12}) is broken, the voltage drop across adjacent resistor (R_7) will increase to 4.53 V quickly. At the moment when its resistance has not yet changed, it has the maximum probability to be broken by Joule heating because of the highest voltage drop and 52% increased power. Similarly, R_2 will have the maximum probability to be destroyed by the 59% increased power at the moment when R_7 is open. As a result, the hot-spot moves perpendicular to the voltage direction during the failure process. Correspondingly, the voltage drops across other resistances decreased obviously, which lead to lower surface temperatures than the hot spot.

ZnO nanoparticles were spin-coated onto the AgNW network to accelerate the transfer of Joule heating. Unlike the AgNW random network with large empty spaces (figure 4(a)), the coated ZnO filled the AgNW interspaces to form nanocomposites (figure 4(b)) with quite good transparency to the eye. The average transparency of PET/AgNW/ZnO (figure 4(c))

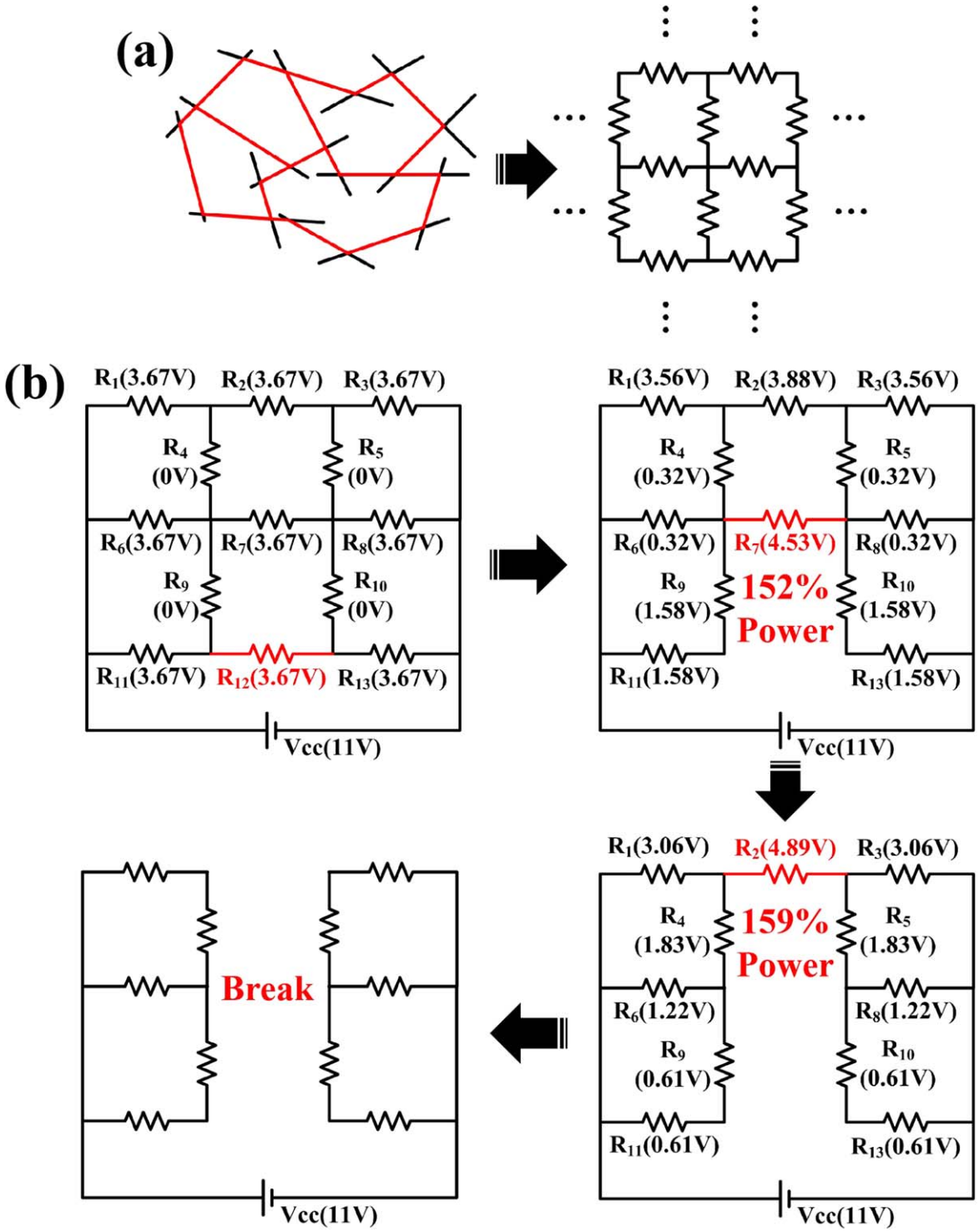

Figure 3. Schematic and equivalent circuit diagram of the AgNW conductive network (a), and the mechanism of the cascading failure with a constant V_{CC} (b).

significantly decreases from 82.8% to 72.7% over blue light (400–480 nm) which was reported to affect the human eye [24], but only drops slightly from 83.3% to 82.7% in other visible light ranges (481–800 nm).

As a transparent thin-film heater, there is a linear relation for data measured in samples with or without ZnO, as shown in figure 5(a). The average temperatures and power densities can be fitted by an equation as follows,

$$T_{ave} = 182.13 \times APD + 25.77 \quad (2)$$

Where APD is the areal power density, and T_{ave} is average temperature. The results show these samples have the same electrical heating efficiency.

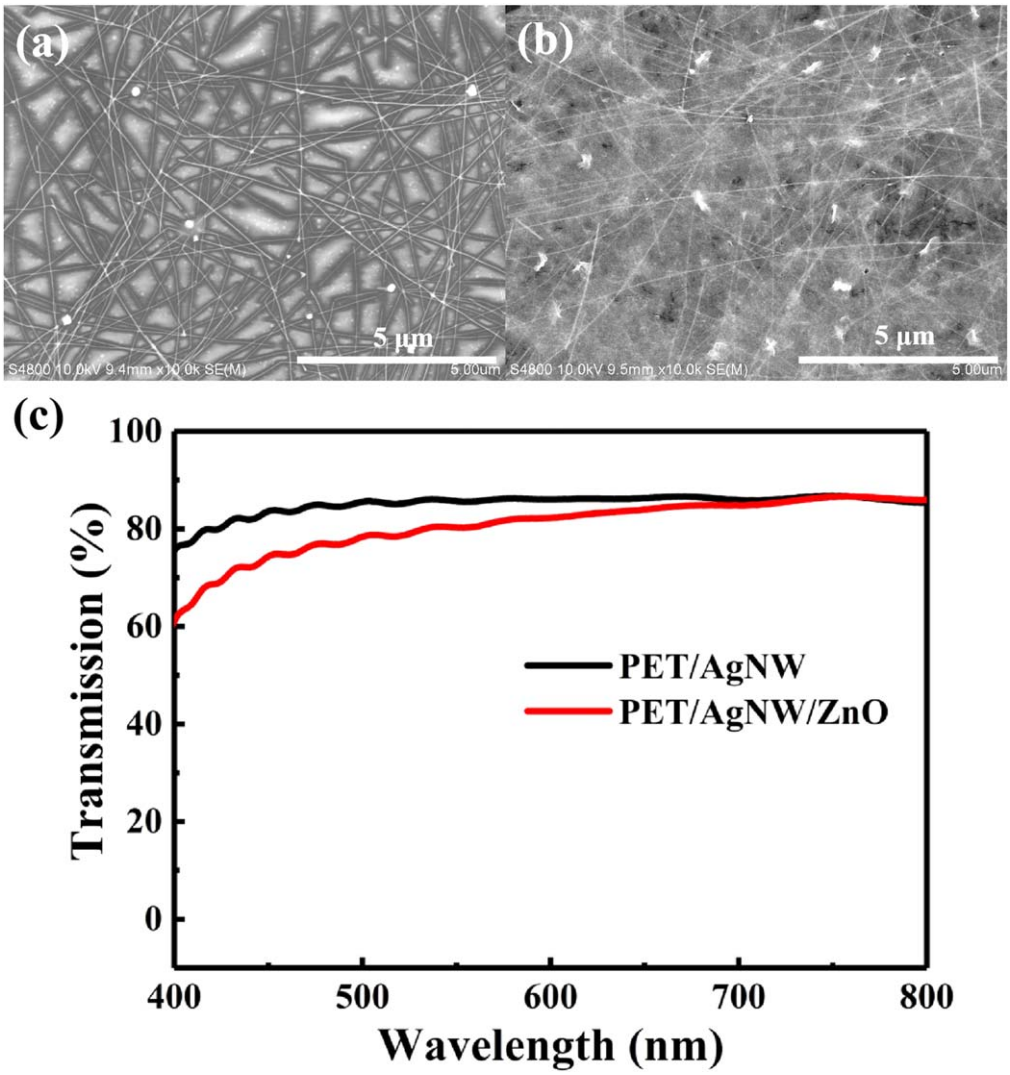

Figure 4. (a), (b) SEM images of AgNW random network and AgNW-ZnO nanocomposite. (c) Comparison of the samples in optical transmittance.

Figure 5(b) shows that the advantage of AgNW-ZnO nanocomposites in Joule-heating uniformity increase obviously at higher temperatures. Take the infrared images of samples at the same average temperature (75.3 °C) as an example (figure 5(c)), the PET/AgNW has the minimum measured temperature of 38.81 °C, while the PET/AgNW/ZnO sample's lowest value is 48.57 °C. But their measured maximum temperature values are similar. Statistics of different temperatures from 9025 points of each sample are shown in figure 5(d), with the temperature distribution histogram and normal distribution curves in 1 °C steps. The results show that 44.51% of the test points on the bare AgNW network have a measured surface temperature higher than 80 °C, while the ratio of AgNW-ZnO is 30.86% at the same average temperature. On the other hand, the standard deviation of bare AgNW (9.79 °C) is 38.47% higher than the AgNW-ZnO nanocomposites (7.07 °C). Considering that the materials have the same electrical heating efficiency, the results show that the Joule-heating homogeneity is improved significantly. The presence of ZnO in the nanocomposites allowing heat to be transfered much faster than in air should be the main reason.

Figure 6(a) displays the highest stable average temperature and areal power density obtained in our experiment (power density larger than these values may lead to breakdown in 2–3 min). The sample with ZnO, which has a highest power density of 0.41 W cm^{-2}, exhibits improved electric heating stability over bare AgNW (0.26 W cm^{-2}). Their maximum average temperatures were correspondingly 97.9 °C (AgNW-ZnO) and 72.2 °C (AgNW). To obtain more details of the properties of a heater based on AgNW-ZnO film, the average current and power density as a function of applied voltage can be found in figure 6(b), as well as the heating and cooling temperature profiles of the AgNW-ZnO nanocomposite heater at various voltages shown in figure 6(c). As a result, a transparent heater based on the PET/AgNW/ZnO thin film can dry water droplets for 40 s at 10 V bias, as shown in figure 6(d).

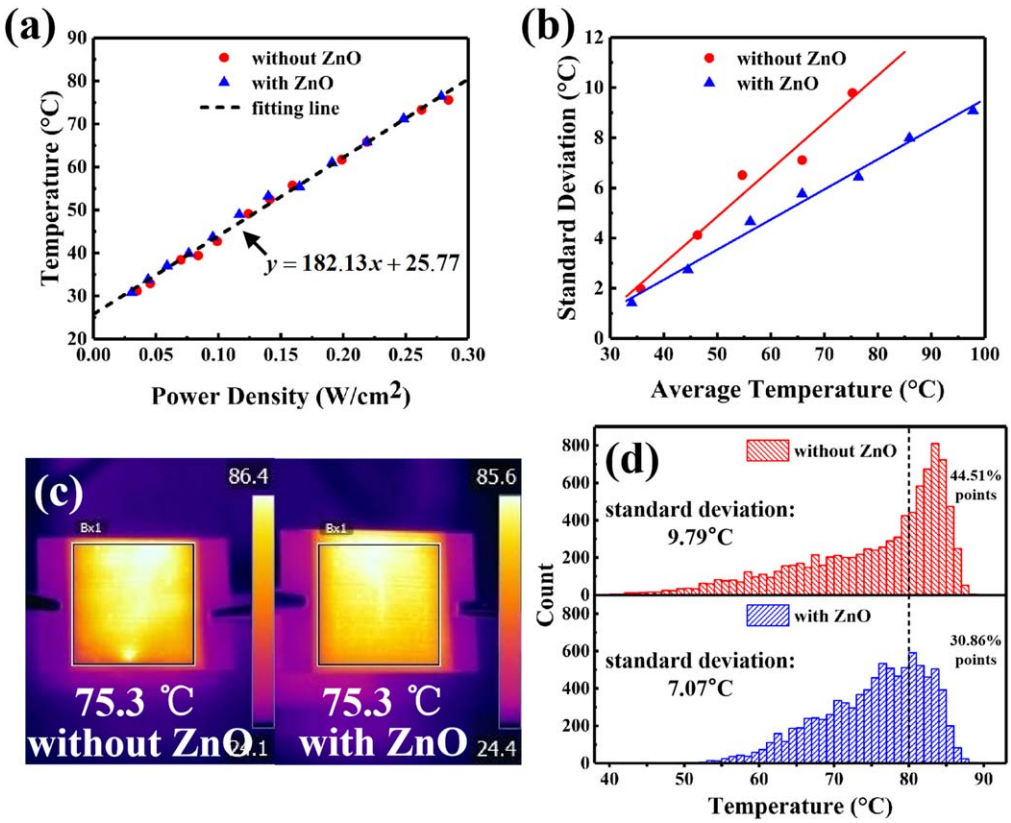

Figure 5. (a) The average temperatures with different power densities. (b) The standard deviations at different temperatures. (c) Comparison of infrared images at the same average temperature. (d) The distribution histograms in 1 °C steps of the samples.

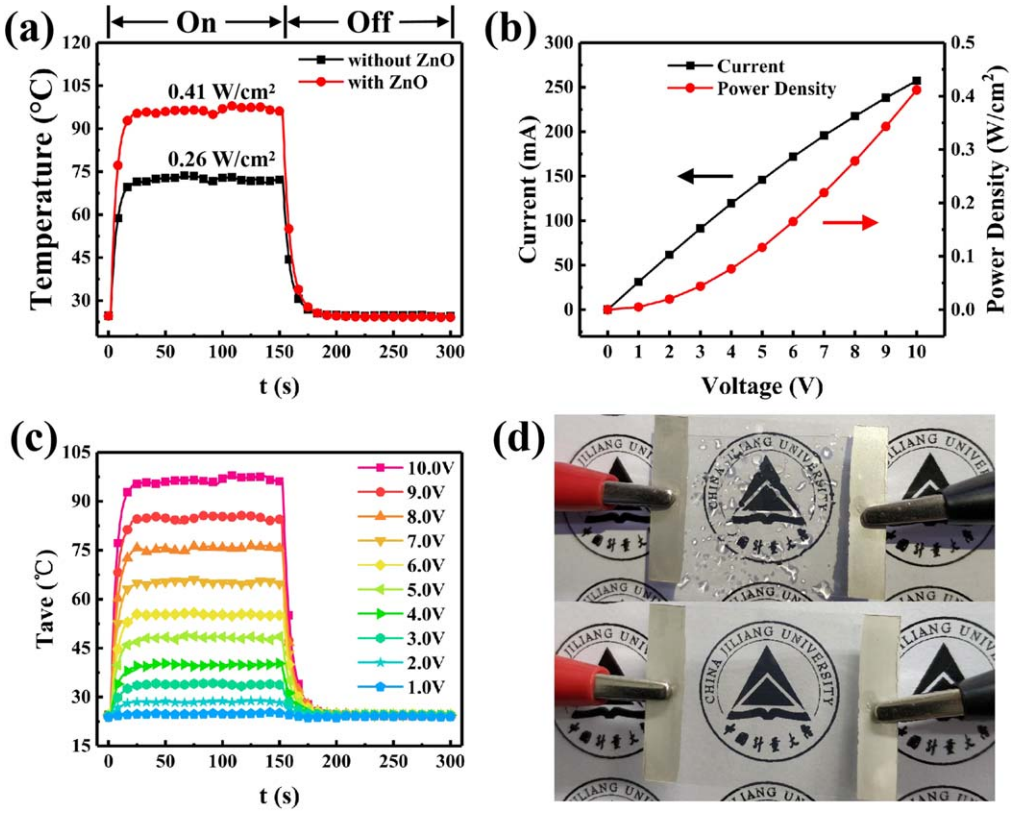

Figure 6. (a) Comparison of the highest stable power density and average temperature. (b) Average current and power density as a function of applied voltage. (c) Heating and cooling temperature profiles of the AgNW-ZnO nanocomposites heater at various voltages. (d) A photo of the PET/AgNW/ZnO thin film heater before (top) and after (bottom) water droplet evaporation at 10 V bias for 40 s.

4. Conclusion

Gravure printed AgNW random networks were improved using solution-processed ZnO for Joule-heating uniformity and stability retaining good transparency for the human eye. The ZnO-AgNW composited heater has an increased advantage in thermal homogeneity at high temperature, which prevents cascading failures from being triggered in the AgNW network. A 57.7% higher power density without failure, as well as a maximum temperature rise from 72.2 °C to 97.9 °C, was obtained in our experiment. This work opens up a new method to study AgNW failures for applications in high-current electronics.

Acknowledgments

The authors acknowledge the financial supports from Youth Innovation Promotion Association, CAS (2019317).

ORCID iDs

Jian Lin https://orcid.org/0000-0002-3037-7023
Qun Luo https://orcid.org/0000-0002-7527-460X

References

[1] Madaria A R, Kumar A and Zhou C W 2011 Large scale, highly conductive and patterned transparent films of silver nanowires on arbitrary substrates and their application in touch screens *Nanotechnology* **22** 245201
[2] Lian L, Xi X, Dong D and He G F 2018 Highly conductive silver nanowire transparent electrode by selective welding for organic light emitting diode *Org. Electron.* **60** 9–15
[3] Han K, Xie M L, Zhang L P, Yan L P, Wei J F, Ji G Q, Luo Q, Lin J, Hao Y Y and Ma C Q 2018 Fully solution processed semi-transparent perovskite solar cells with spray coated silver nanowires/ZnO composite top electrode *Sol. Energy Mater. Sol. Cells* **185** 399–405
[4] Kim D J, Shin H I, Ko E H, Kim K H, Kim T W and Kim H K 2016 Roll-to-roll slot-die coating of 400 mm wide, flexible, transparent Ag nanowire films for flexible touch screen panels *Sci. Rep.* **6** 34322
[5] Krantz J, Stubhan T, Richter M, Spallek S, Litzov I, Matt G J, Spiecker E and Brabec C J 2013 Spray-coated silver nanowires as top electrode layer in semitransparent P3HT:PCBM-based organic solar cell devices *Adv. Funct. Mater.* **23** 1711–7
[6] Jia L C, Yan D X, Liu X F, Ma R J, Wu H Y and Li Z M 2018 Highly efficient and reliable transparent electromagnetic interference shielding, film *Acs Applied Materials & Interfaces* **10** 11941–9
[7] Lu H, Lin J, Wu N, Nie S H, Luo Q, Ma C Q and Cui Z 2015 Inkjet printed silver nanowire network as top electrode for semi-transparent organic photovoltaic devices *Appl. Phys. Lett.* **106** 093302
[8] Peng Y, Du B, Xu X, Yang J, Lin J and Ma C 2019 Transparent triboelectric sensor arrays using gravure printed silver nanowire electrodes *Appl. Phys. Express* **12** 066503
[9] Kholid F N, Huang H, Zhang Y Q and Fan H J 2016 Multiple electrical breakdowns and electrical annealing using high current approximating breakdown current of silver nanowire network *Nanotechnology* **27** 025703
[10] Khaligh H H, Xu L, Khosropour A, Madeira A, Romano M, Pradere C, Treguer-Delapierre M, Servant L, Pope M A and Goldthorpe I A 2017 The Joule heating problem in silver nanowire transparent electrodes *Nanotechnology* **28** 425703
[11] Sannicolo T, Charvin N, Flandin L, Kraus S, Papanastasiou D T, Celle C, Simonato J P, Munoz-Rojas D, Jimenez C and Bellet D 2018 Electrical mapping of silver nanowire networks: a versatile tool for imaging network homogeneity and degradation dynamics during failure *Acs Nano* **12** 4648–59
[12] Bergin S M, Chen Y H, Rathmell A R, Charbonneau P, Li Z Y and Wiley B J 2012 The effect of nanowire length and diameter on the properties of transparent, conducting nanowire films *Nanoscale* **4** 1996–2004
[13] Deignan G and Goldthorpe I A 2017 The dependence of silver nanowire stability on network composition and processing parameters *RSC Adv.* **7** 35590–7
[14] Huang Q J, Shen W F, Fang X Z, Chen G F, Yang Y, Huang J H, Tan R Q and Song W J 2015 Highly thermostable, flexible, transparent, and conductive films on polyimide substrate with an AZO/AgNW/AZO structure *Acs Applied Materials & Interfaces* **7** 4299–305
[15] Chen D, Liang J J, Liu C, Saldanha G, Zhao F C, Tong K, Liu J and Pei Q B 2015 Thermally stable silver nanowire-polyimide transparent electrode based on atomic layer deposition of zinc oxide on silver nanowires *Adv. Funct. Mater.* **25** 7512–20
[16] Khan A, Nguyen V H, Munoz-Rojas D, Aghazadehchors S, Jimenez C, Nguyen N D and Bellet D 2018 Stability enhancement of silver nanowire networks with conformal ZnO coatings deposited by atmospheric pressure spatial atomic layer deposition *Acs Applied Materials & Interfaces* **10** 19208–17
[17] Sun Y, Seo J H, Takacs C J, Seifter J and Heeger A J 2011 Inverted polymer solar cells integrated with a low-temperature-annealed sol-gel-derived ZnO Film as an Electron Transport Layer *Adv. Mater.* **23** 1679–83
[18] Bi S, Li Q, He Z, Guo Q, Asare-Yeboah K, Liu Y and Jiang C 2019 Highly enhanced performance of integrated piezo photo-transistor with dual inverted OLED gate and nanowire array channel *Nano Energy* **66** 104101
[19] Fan S W, Bi S, Li Q K, Guo Q L, Liu J S, Ouyang Z L, Jiang C M and Song J H 2018 Size-dependent Young's modulus in ZnO nanowires with strong surface atomic bonds *Nanotechnology* **29** 125702
[20] Yang X and Daoud W A 2016 Triboelectric and piezoelectric effects in a combined tribo-piezoelectric nanogenerator based on an interfacial ZnO nanostructure *Adv. Funct. Mater.* **26** 8194–201
[21] Zhu L and Zeng W 2017 Room-temperature gas sensing of ZnO-based gas sensor: a review *Sens. Actuators,* A **267** 242–61
[22] He C, Jin N, Yu H R, Lin J and Ma C Q 2019 The electrical sintering and fusing effects of Aerosol-Jet printed silver conductive line *Mater. Lett.* **246** 5–8
[23] Janotti A and Van de Walle C G 2009 Fundamentals of zinc oxide as a semiconductor *Rep. Prog. Phys.* **72** 126501
[24] Tosini G, Ferguson I and Tsubota K 2016 Effects of blue light on the circadian system and eye physiology *Molecular Vision* **22** 61–72 (http://molvis.org/molvis/v22/)